ELSEVIER

Computer Physics Communications 107 (1997) 149–154

Computer Physics Communications

Choice of constants of motion coordinates in numerical solving of the three-dimensional Fokker–Planck equation for tokamaks

T.P. Kiviniemi [a,1], J.A. Heikkinen [b]

[a] *Helsinki University of Technology, Association Euratom–TEKES, P.O. Box 2200, FIN–02015 HUT, Finland*
[b] *VTT Energy, P.O. Box 1604, Association Euratom–TEKES, FIN–02044 VTT, Finland*

Received 23 September 1996; revised 13 August 1997

Abstract

A set of constants of motions is chosen which is found suitable for numerical solving of the three-dimensional neoclassical kinetic equation for low collisionality plasmas in tokamaks. With the chosen set, the constants of motion space is well filled with a unique correspondence to the orbits allowed in the configuration. The numerical treatment of the boundary between the trapped and counter-passing particles becomes more straightforward, because the boundary becomes a function of only one constants of motion coordinate. © 1997 Elsevier Science B.V.

PACS: 19.9; 19.11
Keywords: Fokker–Planck; Tokamak; Neoclassical; Transport

1. Introduction

When the particle and energy confinement in a fusion reactor are considered, transport processes in a toroidal configuration are of great interest. Within a so-called neoclassical theory of transport [1], various important experimentally observed mechanisms like the decrease in conductivity along field lines, the increased pinch effect, and the generation of a bootstrap current have been predicted. The transport coefficients obtained from this theory also give the minimum particle and heat flux in a real experiment. The neoclassical transport resulting from collisions in an axi- or nonaxisymmetric toroidal plasma with an arbitrary cross section can nowadays be calculated to a good accuracy [1,2] when the particle drift-trajectories do not deviate significantly from constant-density and constant-temperature surfaces. Here, also various analytical models exist under various approximations. However, accurate modelling of drift-trajectories has been found important in the simulation of the transport of the fusion products and nonthermal ions. In order to incorporate the finite orbit effects, a direct modelling of the transport processes with an orbit following Monte Carlo method has appeared [3] in various applications. However, in this technique, it is complicated to preserve momentum conservation in collisions, and the good accuracy necessitates very costly numerical calculations. To model the plasma behaviour correctly in thermonuclear plasmas, in which the fast ion populations with wide drift-trajectories are an important component, solution methods for a more complex kinetic equation than the drift-kinetic equation [1] in a thin-trajectory approximation are called for. To satisfy the momentum conservation, a nonlin-

[1] E-mail: Timo.Kiviniemi@hut.fi

PII S0010-4655(97)00106-9

ear collision operator [1] has to be included.

Recently, a three-dimensional nonlinear kinetic equation for low collisionality axisymmetric tokamak plasmas with consistent consideration of neoclassical effects has been obtained using a formalism based on noncanonical variables [4]. The method allows treatment of large drift-trajectory widths and large inverse aspect ratios, conserves momentum in collisions and is suitable for computer modelling of neoclassical transport of thermal and nonthermal distributions. The study of phenomena arising from non-Maxwellian distributions is important, in particular, in the study of plasma heating and current drive by Ohmic or radio-frequency heating, and in the study of the effects, confinement and heating, by the energetic fusion products. The noncanonical variables have been shown in Refs. [4,5] to be more convenient for numerical solution and physical interpretation than canonical variables. The nonlinear kinetic equation in general coordinates can be written as

$$\frac{\partial f}{\partial t} = \frac{1}{J} \sum_{n=1,2,3} \frac{\partial}{\partial \bar{x}^n} \left[\sum_{m=1,2,3} \left(A_{nm} \frac{\partial f}{\partial \bar{x}^m} \right) + B_n f \right], \tag{1}$$

where f is the distribution function, $\bar{x} \equiv (\gamma_0, v_0, \lambda)$, J is the Jacobian and the detailed forms of the collisional coefficients A_{nm} and B_n are given in [4].

In an axisymmetric tokamak, three constants of motion (COM) are required to completely characterize the guiding-centre motion of a particle. Three conservation laws, conservation of total particle energy $\epsilon = mv^2/2 + q\Phi$, conservation of the magnetic moment $\mu = mv_\perp^2/2B$, and conservation of the toroidal momentum $p_{\mathrm{tor}} = mRv_\parallel B_{\mathrm{tor}}/B - q\psi$ fix the trajectory of the particle in phase space. Here, q and m are the particle charge and mass, respectively, Φ is the electrostatic potential, v is the velocity, $v_\perp$ and $v_\parallel$ are the perpendicular and parallel components of the velocity with respect to magnetic field $\boldsymbol{B}$, respectively. B_{tor} is the toroidal component of the magnetic field, ψ is the poloidal flux of the magnetic field and R is the major radius. In principle, the orbits could be represented in $\epsilon, \mu, p_{\mathrm{tor}}$-space, but for the numerical simulation this set is inconvenient. For the 'good' set of constants of motion, it is required that (a) coordinates should be physically meaningful, (b) representation should be unique in the sense that a given point in the COM space corresponds to one and only one orbit, and (c) phase space should be well filled [6]. In $\epsilon, \mu, p_{\mathrm{tor}}$-representation, the configuration space and velocity space are mixed, there is an indeterminacy of the sign of particle pitch $v_\parallel/v = \cos\theta$, and the phase space proves to be mostly empty and multi-sheeted.

A new choice for the variables was suggested in [4]. Instead of ϵ, coordinate v_0 is chosen, which is the speed corresponding to the total energy including electrostatic potential. As a spatial coordinate, a convenient variable is γ_0 being the flux surface label on the innermost point of the drift trajectory for passing particles and at the bounce point for trapped particles. As the third coordinate, the pitch angle θ_0 at the outermost point of the trajectory was used in [4] and has been programmed in the FPP code [7], but here it is found to be inconvenient, because the boundary between trapped and counter-passing particles (TPB) is not continuous with respect to θ_0 and the numerical treatment of this would be complicated. Also, the requirement that the space is well filled is not satisfied, because the trapped particles have only positive values of $\cos\theta_0$ due to the fact that negative $\cos\theta_0$ values at the *outermost* point of the orbit occur only for the counter-passing particles. This leaves a large region in the middle of the COM-space empty (black region in Fig. 1a).

Another choice for solving a Fokker–Planck equation in 3D phase space was suggested by Rome and Peng [6]. Here, the pitch and the flux surface coordinates were determined at the position where the poloidal flux function along the guiding-centre orbit obtains its maximum. For this choice of the coordinates, the boundary between counter-passing and trapped particles is continuous neither in pitch angle nor in flux surface coordinate. Also the forbidden region inside the COM-space is larger and more cumbersome to treat numerically.

In order to avoid the above-mentioned problems, we adopt here the coordinates v_0 and γ_0 as in Ref. [4], but for the third COM-coordinate we suggest

$$\lambda = \begin{cases} \theta^i(B_{\max}, \xi^i = \pi), & \text{for passing particles,} \\ \xi^i(B_{\max}, \theta^i = \pi/2), & \text{for trapped particles,} \end{cases}$$

which is the pitch angle θ^i in the *innermost* point of the trajectory for passing particles and the poloidal angle ξ^i at the bounce point for trapped particles. With

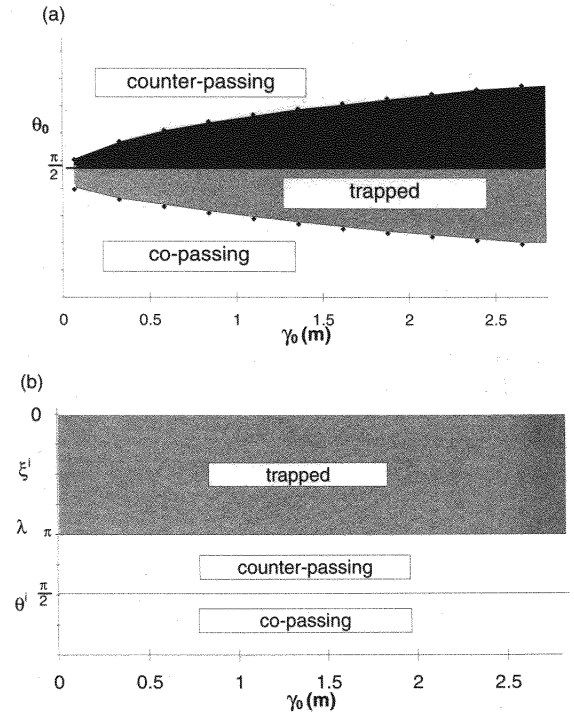

Fig. 1. Trapped and passing regions (a) in (γ_0, θ_0) space and (b) in (γ_0, λ) space, in which the distribution function at $\xi^i = \pi$ is continuous to the one at $\theta^i = \pi/2$.

this choice, the requirement of the well-filled space is satisfied, which can be seen in Fig. 1b, and the treatment of the trapped-passing boundary is simpler, because γ_0 and λ are defined at the same point and both are continuous across the TPB. It is also important to note that the trapped-passing boundary with present coordinates is independent of γ_0 and v_0 which makes the differencing straightforward.

2. Solving the trajectories

In Ref. [4] seven transcendental algebraic equations were needed to solve for γ, v and θ, being the local values of the flux surface label, velocity and pitch angle, respectively, and four subsidiary variables γ^o, v^o, v^i and ξ^i or θ^i for a given set γ_0, ξ, v_0 and θ_0. Here superscripts i and o denote the innermost and outermost values of the variables, respectively. In our new coordinates only four equations

$$\frac{mv_0^2}{2} = \frac{mv^2}{2} + q\Phi(\gamma) = \frac{m(v^i)^2}{2} + q\Phi(\gamma_0)\,, \tag{2}$$

$$\frac{mv^2\sin^2\theta}{2B(\gamma,\xi)} = \frac{m(v^i)^2\sin^2\theta^i}{2B(\gamma_0,\xi^i)}\,, \tag{3}$$

and

$$\frac{mv\cos\theta F}{B(\gamma,\xi)} - q\psi(\gamma) = \frac{mv^i\cos\theta^i F}{B(\gamma_0,\xi^i)} - q\psi(\gamma_0)\,, \tag{4}$$

are needed with v^i being the only subsidiary variable and we have defined $F = RB_{\mathrm{tor}}$. Now, we can solve for v from Eq. (2) and θ from Eq. (3), both as a function of γ, ξ and the COM coordinates, and put them into Eq. (4) where we can iterate the value of γ and after that, other local coordinates can be easily solved.

3. Trapped-passing boundary

In differencing Eq. (1), the grid for λ, according to Fig. 1b, is given by $\lambda_j = j\pi/N$, $j = 0, \ldots, N$, in the passing particle regime, and by $\lambda_j = (M+N-j)\pi/M$, $j = N, \ldots, N+M$, in the trapped particle regime. As is evident from this, the same numerical value can appear twice in the grid. The corresponding values of θ^i, ξ^i at the grid points are found according to Table 1, where N and M are the number of different θ^i and ξ^i values, respectively, and N is assumed to be even. Typically, $M \geq 5$ and $N \approx M$ gives accurate results for the particle and energy fluxes. The three regions – co-passing, trapped and counter-passing – are connected via the TPB layer. The distribution function at the grid point λ_{N+1} in the trapped regime is continuous to the one at $\lambda_{N/2}$ in which $\xi^i = \pi$ and $\theta^i = \pi/2$. In Fig. 1b, the co-passing, counter-passing and trapped regions are limited by the TPB and by the boundaries at $\theta^i = 0$, $\theta^i = \pi$ and $\xi^i = 0$, respectively, in which the particle flux becomes zero. Differencing over the TPB layer needs a more careful consideration. For convenience, let us consider the one-dimensional case,

$$\begin{aligned}\frac{\partial f_k}{\partial t} &= \frac{1}{J}\frac{\partial}{\partial\lambda}\left(A_k\frac{\partial f_k}{\partial\lambda} + B_k f_k\right)\\ &\doteq \frac{1}{J}\left[\left\{\frac{A_{k+1/2}}{\Delta\lambda^2}(f_{k+1} - f_k) + \frac{B_{k+1/2}}{\Delta\lambda}f_{k+1/2}\right\}\right.\\ &\quad\left.-\left\{\frac{A_{k-1/2}}{\Delta\lambda^2}(f_k - f_{k-1}) + \frac{B_{k-1/2}}{\Delta\lambda}f_{k-1/2}\right\}\right]\end{aligned}$$

Table 1
Corresponding values of θ^i, ξ^i at the grid points

					λ	θ^i	ξ^i				
λ:	λ_0	λ_1	$\cdots$	$\lambda_{N/2-1}$	$\lambda_{N/2}$		TPB	$\lambda_{N/2+1}$	$\cdots$	λ_{N-1}	λ_N
θ^i:	0	$\frac{\pi}{N}$	$\cdots$	$\frac{(N/2-1)\pi}{N}$		$\pi/2$		$\frac{(N/2+1)\pi}{N}$	$\cdots$	$\frac{(N-1)\pi}{N}$	π
ξ^i:	π	π	$\cdots$	π			π	π	$\cdots$	π	π
					λ_{N+1}	$\pi/2$	$\frac{(M-1)\pi}{M}$				
					$\vdots$	$\vdots$	$\vdots$				
					λ_{N+M-1}	$\pi/2$	$\frac{\pi}{M}$				
					λ_{N+M}	$\pi/2$	0				

Co-passing *Counter-passing* *Trapped*

$$= \frac{1}{J}[\{\text{flux from } f_{k+1} \text{ to } f_k\} - \{\text{flux from } f_k \text{ to } f_{k-1}\}]/\Delta\lambda\,, \quad (5)$$

ignoring the γ_0 and v_0 derivatives. Here, grid spacing is $\Delta\lambda = \pi/N$ in the passing region and $\Delta\lambda = \pi/M$ in the trapped region. We notice that the change in the distribution function f in the grid point k is just the difference of incoming and outgoing fluxes divided by the distance between the grid points. However, when the TPB point is considered, derivative over the θ^i region can be done normally, but also the contribution of the trapped region has to be taken into account. In our coordinates the coefficients $A_{N+1/2}$ and $B_{N+1/2}$ connect the distributions f_{N+1} and $f_{N/2}$ (not f_N), and the flux from the trapped region to the TPB layer is

$$\bar{j}_{N+1/2} = \frac{1}{J}\left[\frac{A_{N+1/2}}{\Delta\lambda}(f_{N+1} - f_{N/2}) + B_{N+1/2} f_{N+1/2}\right].$$

The interaction between the three regions of different orbit topologies can be described by

$$\begin{aligned}\frac{\partial f_{N/2}}{\partial t} = \frac{1}{J}\Bigg[&\frac{A_{N/2+1/2}}{\Delta\lambda^2}(f_{N/2+1} - f_{N/2}) \\ &+ \frac{B_{N/2+1/2}}{\Delta\lambda} f_{N/2+1/2} \\ &- \frac{A_{N/2-1/2}}{\Delta\lambda^2}(f_{N/2} - f_{N/2-1}) \\ &- \frac{B_{N/2-1/2}}{\Delta\lambda} f_{N/2-1/2} \\ &+ \frac{A_{N+1/2}}{\Delta\lambda^2}(f_{N+1} - f_{N/2}) \\ &+ \frac{B_{N+1/2}}{\Delta\lambda} f_{N+1/2}\Bigg], \end{aligned} \quad (6)$$

which also guarantees that the condition

$$f_\alpha(t, \overline{X}_+) = f_\alpha(t, \overline{X}_-) = f_\alpha(t, \overline{X}_{\rm tr}) \quad (7)$$

given in [4] is fulfilled. Here, "+", "−", and "tr" denote the boundary points taken from the co-passing, counter-passing and trapped regions, respectively. The formalism presented in [4] to get Eq. (1) by averaging over the "fast" coordinates (poloidal, toroidal and gyroangles) is not valid near the trapped passing boundary, where characteristic times for motion over these coordinates become comparable to the Coulomb relaxation time. In our new coordinate system the diffusion coefficient $A_{\lambda\lambda}$ at the TPB goes to infinity as

$$\lim_{\theta^i \to \pi/2} A_{\theta^i\theta^i} \sim \tan^2\theta^i \to \infty\,,$$

$$\lim_{\xi^i \to \pi} A_{\xi^i\xi^i} \sim 1\Big/\frac{\partial B}{\partial \xi^i} \to \infty\,,$$

where the second equation is true only in up–down symmetric plasmas. From the infinite $A_{\lambda\lambda}$ follows that $\partial f/\partial\lambda = 0$ at the TPB, which is consistent with Eq. (7).

4. Benchmark test

The outward flux of the ions calculated by the code using the new set of COM coordinates is here compared with the analytical estimate, which is calculated in the banana region in a tokamak with circular flux surfaces and by neglecting the effect of the ambipolar radial electric field [4]. Assumptions are that the inverse aspect ratio $\epsilon = \gamma/R$ is small, distributions are close to Maxwellian and that deviations of the drift-trajectories from flux surfaces are small. The expression for the local radial particle flux is

$$\Gamma_i = -2\pi \int_0^{\infty} \int_{\theta_{TPB}^{(1)}}^{\theta_{TPB}^{(2)}} j_\perp v^2 \sin\theta \, d\theta \, dv \,, \tag{8}$$

where the pitch angle has been restricted to trapped particles, as to lowest order in ϵ, the flux of passing particles is zero, and the flux through the magnetic surface labeled γ is approximately

$$j_\perp \approx \frac{A_{11}}{J} \frac{\partial f_M}{\partial \gamma_0} \,, \tag{9}$$

assuming that the contributions of other coefficients vanish in integration. Contributions of the other ion species and electrons have been neglected. The analytical estimates have been calculated from these formulas using predetermined radial shapes for the distribution. The code calculations have been done using the complete form

$$j_\perp = \bar{j} \cdot \boldsymbol{n} = \frac{1}{J|\nabla\gamma|} \sum_{n=1,2,3} \frac{\partial \gamma}{\partial \bar{x}^n} \times \left[\sum_{m=1,2,3} \left(A_{nm} \frac{\partial f}{\partial \bar{x}^m} \right) + B_n f \right] , \tag{10}$$

for the flux with $\bar{x} \equiv (\gamma_0, v_0, \lambda)$ and including also the contribution of the background electrons.

In the calculations, parameters $a = 2.8$ m, $B = 6.157$ T, $I = 15$ MA, $n_{D,e,0} = 0.4 \times 10^{20}$ m^{-3} and $T_{D,e,0} = 10$ keV are chosen for the minor radius, magnetic field, plasma current, and plasma deuteron and electron density and temperature, respectively. The plasma density, temperature and current density are assumed to have radial dependencies $n, T, I = n_0, T_0, I_0 \times (1 - \gamma^2/a^2)^{\alpha_{n,T,I}}$ with $\alpha_n = \alpha_T = 0.5$ and $\alpha_I = 1$. Numerical results are given for the initial deuterium distribution $t = 0$ and for $t = 0.3$ s, which do not differ much, because the deuterons already have the background temperature in the beginning of the time evolution. The grid size is $(N_{\gamma_0}, N_{v_0}, N_\lambda) = (20,25,16)$. The results have been presented in the regime, where further increasing the number of grid points changes the results less than two percent.

In Fig. 2a, a good agreement between the analytical and numerical results can be seen. In calculating the analytical estimate, the assumption of a small inverse aspect ratio was done. For this reason, we can see that the analytical result, although in good agreement with the numerical one near the axis, begins to diverge when going towards the edge of plasma. In Fig. 2b, the ratio between the numerical and analytical result is presented as a function of the local aspect ra-

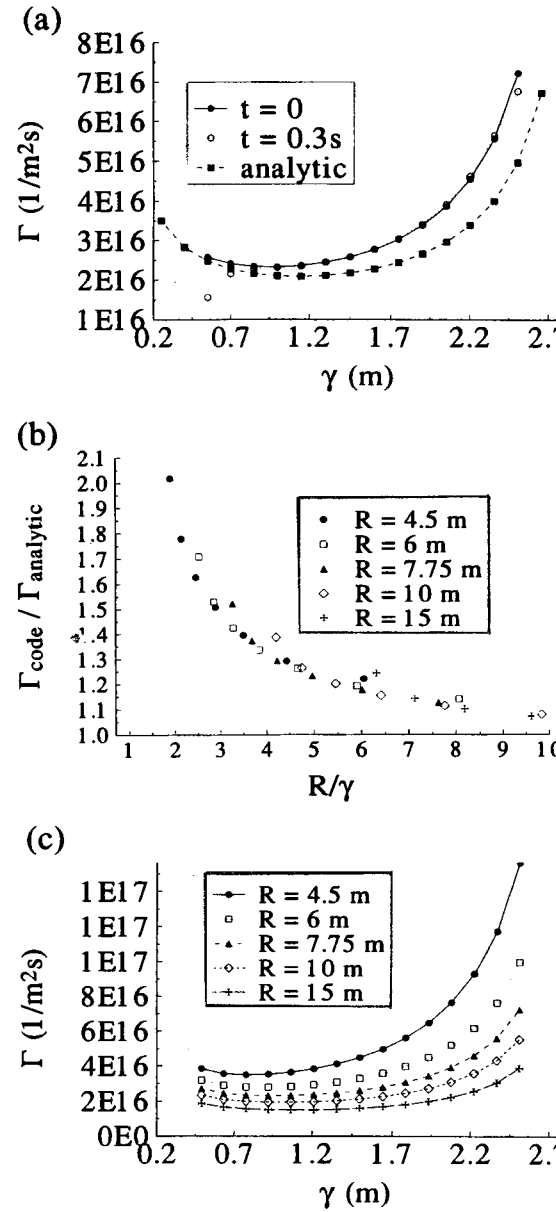

Fig. 2. (a) Particle flux Γ_i for $R = 7.75$ m; (b) ratio between the numerical and analytical result as a function of aspect ratio; and (c) particle flux for five different major radii R with $a = 2.8$ m.

tio R/γ from five different tokamaks with fixed minor radius $a = 2.8$ m and with different major radii R. It can be seen that the analytical flux strongly underestimates the true flux obtained from the numerical result for small aspect ratios $R/\gamma \leq 5$ and thus the validness of the large aspect ratio approximations for the neoclassical fluxes is clearly limited. In Fig. 2c, the neoclassical particle flux calculated numerically from the initial distribution is presented for the cases shown in Fig. 2b as a function of γ. The flux becomes essentially larger near the plasma edge where the density and temperature gradients are large. Here, the requirements to keep the accuracy are made more significant than elsewhere at weak gradient regimes. A much more dense grid locally in γ is required for $0.9 < \gamma/a < 1$ in our example to keep the same accuracy.

The performance of the code using the new coordinate system has been measured on the IBM 9076 SP1 computer. The critical parameters for the total CPU-time usage are the size of the distribution grid $(N_{\gamma_0}, N_{\iota_0}, N_\lambda)$, the number of integration points N_{3D} in the three-dimensional integral over the fast variables and the number of background particle species N_{spec}. For the time advancement of the distribution function, a two cycle six stage operator splitting scheme [7,8] is used. The estimate of the runtime of the code is

$$t_{run} \approx N_{\gamma_0} N_{\iota_0} N_\lambda [2.4 N_{3D} N_{spec} + N_{steps}(2N_{\gamma_0} + N_\lambda)] \times 10\ \mu s, \quad (11)$$

where N_{steps} is the number of time steps needed. If time evolving collisional coefficients are used, the first term inside the brackets has to be multiplied with N_{steps} meaning a huge increase of runtime. Possible decrease in computation time when compared to previous treatment [7] is due to reduction in the number of needed grid points to get accurate results. Also, solving the tractories in real space for given COM space grid points is more efficient because only four equations are needed instead of seven. A corresponding law for memory size allocation is more difficult to give. Memory occupation is mainly dictated by the grid size and the number of points in integration over the trajectory.

5. Conclusions

A new choice of constants of motion coordinates has been found to be suitable for the modelling of the different orbit topologies with the kinetic equation for tokamaks. The treatment of the TPB has been found to be simpler when compared to previous approaches. Solving the local coordinates for the trajectory defined by the COM coordinates is easier, because only four equations and variables are needed here instead of seven in Ref. [4]. The code using the new set of COM variables has been tested by comparing the outward neoclassical ion flux to the analytical estimates, and a good agreement within the range of validity of the analytical model has been found. The numerical method presented here is suitable for the study of neoclassical transport of electrons and ions in weakly collisional (banana regime) axisymmetric toroidal plasmas of arbitrary cross section in the presence of thermal and nonthermal plasma components with momentum conservation in collisions and in the presence of finite drift-trajectory widths. The applications of the present code are of particular interest for the heating and current generation by energetic fusion products and by auxiliary heating methods as well as for the studies of the loss of fast particles from the plasma configuration and for calculations of the ambipolar radial electric field in the presence of nonambipolar loss of some plasma component.

References

[1] F.L. Hinton, R.D. Hazeltine, Rev. Mod. Phys. 48 (1976) 239.
[2] M. Taguchi, Phys. Fluids B 4 (1992) 3638.
[3] R.E. Potok, P.A. Politzer, L.M. Lidsky, Phys. Rev. Lett. 45 (1980) 1328;
A.H. Boozer, G. Kuo-Petrovic, Phys. Fluids 24 (1981) 851;
R.H. Fowler, J.A. Rome, J.F. Lyon, Phys. Fluids 28 (1985) 338;
H.E. Mynick, Phys. Fluids 25 (1982) 325;
W. Lotz, I. Nürenberg, Phys. Fluids 31 (1988) 2984;
C.D. Beidler, W.N.G. Hitchon, D.L. Grekov, A.A. Shinshkin, Nucl. Fusion 30 (1990) 405.
[4] Z.S. Zaitsev, M.R. O'Brien, M. Cox, Phys. Fluids B 5 (1993) 509.
[5] L.M. Hively, G.H. Miley, J.A. Rome, Nucl. Fusion 21 (1981) 1431.
[6] J.A. Rome, Y-K.M. Peng, Nucl. Fusion 19 1979) 1193.
[7] M.R. O'Brien, M. Cox, C.D. Warrick, Z.S. Zaitsev, JET-P(92)42.
[8] G.I. Marchuk, Methods of Numerical Mathematics, 2nd ed. (Springer, New York, 1982).